Send Orders for Reprints to reprints@benthamscience.ae

Current Medicinal Chemistry, 2018

Metabolomics-guided isolation of anti-trypanosomal compounds from endophytic fungi of the mangrove plant *Avicennia lanata*

Noor Wini Mazlan*[a,b], Rothwelle Tate[a], Yusnaini Md. Yusoff[a], Carol Clements[a], and RuAngelie Edrada-Ebel*[a]

[a] *Strathclyde Institute of Pharmacy and Biomedical Sciences, University of Strathclyde, The John Arbuthnott Building, 161 Cathedral Street, Glasgow G4 0RE, Scotland;* [b]*Chemistry and Environmental Analysis, School of Marine and Environmental Sciences, Universiti Malaysia Terengganu, 21030 Kuala Terengganu, Terengganu, Malaysia*

Abstract: Endophytic fungi have been explored not just for their ecological functions but also for their secondary metabolites as a new source of these pharmacologically active natural products. Accordingly, many structurally unique and biologically active compounds have been obtained from the cultures of endophytic fungi. *Fusarium* sp. and *Lasiodiplodia theobromae* were isolated from the root and stem of the mangrove plant *Avicennia lanata*, respectively, collected from Terengganu, Malaysia. High-resolution mass spectrometry and NMR spectroscopy were used as metabolomics profiling tools to identify and optimize the production of bioactive secondary metabolites in both strains at different growth stages and culture media. The spectral data was processed by utilizing a quantitative expression analysis software, the modified Mzmine 2.10, an in house MS-Excel macro coupled with Antimarin (Antibase and Marinlit) and Dictionary of Natural Products databases for dereplication studies. The investigation for the potential bioactive metabolites from a 15-day rice culture of *Fusarium* sp. yielded four 1,4-naphthoquinone with naphthazarin structures (**1-4**). On the other hand, the endophytic fungus *L. theobromae* grown on the 15-day solid rice culture produced dihydroisocoumarins (**5** to **8**). All the isolated compounds (**1** to **8**) showed significant activity against *Trypanosoma brucei brucei* with MIC values of 0.32-12.5 μM. Preliminary cytotoxicity screening against normal prostate cells (PNT2A) was also performed. All compounds exhibited low cytotoxicity, with compounds **3** and **4** showing the lowest cytotoxicity of only 22.3% and 38.6% of the control values at 100

XXX-XXX/14 $58.00+.00

μg/mL, respectively. Structure elucidation of the isolated secondary metabolites was achieved using 2D-NMR and HRESI-MS as well as comparison with literature data.

Keywords: Endophytic fungi, dereplication, metabolomics, mass spectrometry, multivariate analysis.

* Strathclyde Institute of Pharmacy and Biomedical Sciences

University of Strathclyde, The John Arbuthnott Building

161 Cathedral Street, Glasgow G4 0RE, UK

Tel:+44(0)141 548 5968 Fax:+44(0)141 552 2562; Chemistry and Environmental Analysis, School of Marine and Environmental Sciences, Universiti Malaysia Terengganu, 21030 Kuala Terengganu, Terengganu, Malaysia; Tel/Fax: +609 668 3235, +609 668 3193; E-mails: ruangelie.edrada-ebel@strath.ac.uk; noorwini@umt.edu.my.

1. INTRODUCTION

Endophytes are defined as microorganisms that live inter- and/or intra-cellular in plant tissues for a short or prolonged period without producing any visible disease symptoms [1]. The endophytic fungi also produce different group of compounds to promote plant growth and protect the plant from environmental stress or animal predation. For mutualism, these microorganisms receive thriving space within the host plant [2]. Unique bioactive metabolites produced by endophytes are not only advantageous for the plant itself but also possess high potential for new medicines, which will be able to treat certain diseases in humans. They may also be utilized in functional foods. The first report on mangrove fungi was in 1955 when Cribb did an isolation work on mangrove roots from Australia [3].

Recently, the number of studies on unique and biologically active compounds produced by endophytic fungi especially from marine sources has increased due to advances in dereplication and chromatographic methodologies.

1.1. Dereplication studies

The dereplication method is a process for screening the known metabolites from the crude extracts before further scale-up or isolation work was undertaken, in order to avoid repetitive work that has already been earlier reported in the literature. High-resolution electrospray ionisation-liquid chromatography-mass spectrometry (HRESI-LCMS) data from both positive and negative ionization modes were subjected to dereplication of the secondary metabolites found in the crude extracts. The

dereplication process, coupled with databases such as the Dictionary of Natural Products (DNP) and Antimarin, assisted in the isolation and purification steps of the bioactive natural product.

1.2. Metabolomics

Metabolomics is a technology of integral experimental analysis of metabolites which includes four basic steps: 1) sample preparation and extraction, 2) data acquisition (analysis of the extracts), 3) data mining including data processing and multivariate analysis and 4) metabolite identification or dereplication [4]. It has been applied in multidisciplinary areas to identify and quantify metabolites such as in molecular and cell biology, functional genomics, chemical toxicology, pathology, chemical ecology, drug metabolism, disease progression and natural products chemistry of terrestrial plants, marine organisms and their associated-microorganisms [5-7]. A pioneer study using the 'metabolite profiling' concept was published in the early 1970s [8, 9] which reported the analysis of steroids derivatives, acids, and neutral and acidic urinary drug metabolites using gas chromatography-mass spectrometry (GC-MS). In natural products research, the term 'metabolite' refers to a group of small molecules with a molecular weight of <1000 Da. These are classified into primary and secondary metabolites. Primary metabolites, which include amino acids, lipids and carbohydrates, refer to molecules that are required to support the growth or function of an organism via normal metabolic process. Secondary metabolites, including polyphenols, alkaloids, terpenes, polyketides and hormones are molecules related to signaling mechanisms for an organism's defense and survival [10]. Some of these compounds possess potent activity in certain targeted biological tests, making them valuable in drug discovery and development. Metabolite profiling of the active metabolites in crude extracts of natural sources is supported by dereplication in which the novel compounds from the active groups are differentiated from known compounds which have been studied previously [11]. Therefore, a comprehensive analysis on different metabolites in complex mixtures can be achieved using several alternative methods such as "metabolite (or metabolic) fingerprinting," "metabolite profiling" and "metabolite target analysis". The term "metabolic" is used mostly in drug research; it is commonly used to describe the metabolic fate of an administered drug [12]. Therefore, metabolomics tools were used to accelerate the identification of potential bioactive components from the crude extracts. Using metabolomics and bioassay-guided isolation work to search for the bioactive secondary metabolites against the protozoan *Trypanosomal brucei brucei* (*T. b. brucei*) S427, the organic crude extract of endophytic fungi *Fusarium* sp. afforded four naphthazarin-related naphthoquinones; namely anhydrofusarubin (**1),** javanicin (**2**), dihydrojavanicin (**3**), and solaniol (**4**). The investigation for other potential bioactive compounds from *Lasiodiplodia theobromae* afforded dihydroisocoumarin congeners, which included *trans* (**5)** and *cis* (**6**) 4,8-dihydroxy-3-methylisochroman-1-one, 5-hydroxymellein (**7**) as well as mellein (**8**) (Figure 1) after a series of chromatographic purification.

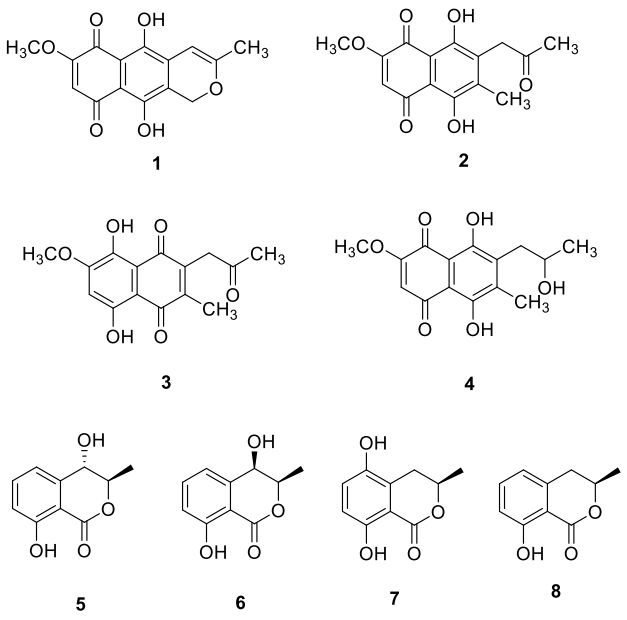

Figure 1. Compounds isolated from the endophytes of the mangrove plant *Avicennia lanata***.**

1.3. Multivariate analysis in metabolomics

The complex data generated from liquid chromatography-mass spectrometry (LC-MS) and nuclear magnetic resonance spectroscopy (NMR) were subjected to statistical multivariate analysis (MVA) to extract the greatest amounts of useful information from the data. A basic unsupervised principal component analysis (PCA) was used as the first step for MVA to reduce data dimensionality while retaining data quality, followed by different supervised MVA models depending on the specific data quality and research objectives [13]. In PCA, major sample components were structured to represent data variance in a two or three-dimensional coordinate scheme. This approach disclosed the grouping model of samples and visualized the discriminant outliers which may indicate potential novel bioactive natural products which can be targeted for subsequent analysis [14]. One of the broadly used supervised MVA was partial least squares (PLS); it related a data matrix containing independent variables from samples, such as spectral intensity values (an X matrix) to a matrix containing dependent variables (e.g. measurements of response, such as toxicity scores) for those samples (a Y matrix) [15]. OPLS was also combined with discriminant analysis (DA) to establish the optimal position to place a discriminant surface which best separated the classes. In the final step of the metabolomics approach, the selected unique biomarkers were interpreted to putatively identify the bioactive metabolites using databases like DNP and Antimarin.

1.4 Human African trypanosomiasis

Natural products research has an important role in the discovery of various biologically active substances of natural origin for potential new drugs. Human African trypanosomiasis is a neglected disease that requires international efforts in the development of new potential alternative drugs. Many of the affected rural populations have limited access to appropriate healthcare, and the production of anti-trypanosomal drugs is costly. Moreover, the available drugs used for the treatment of trypanosomiasis depend on the sub-species of the trypanosomes as well as the stage of the disease. The requirement for drugs that are able to cross the blood brain barrier to get into contact with the parasites is also a major challenge in drug design, hence some drugs are difficult to administer, are toxic, and cause adverse drug reactions [16, 17]. The current situation necessitates the development of new, effective, cheap and safe remedies to combat the trypanosomiasis. Even now, there are no drugs of natural origin available commercially that can treat the disease. However, society has typically relied on traditional medicine from natural sources to heal a wide range of diseases [18-20] and indeed, previous studies on naphthoquinone metabolites which have been isolated from several plant sources have revealed promising anti-trypanosomal activity [21-23]. This has driven us to intensify our search for potential anti-trypanosomal agents from natural sources.

In this phytochemical study, a metabolomics approach was used to target the anti-trypanosomal active secondary metabolites as well as in preliminary screening the production of these target metabolites by the plant's endophytic fungi. The main aims in the present work were to isolate secondary metabolites for anti-trypanosomal derived drugs from the endophytic fungi from *Avicennia. lanata* by utilizing metabolomics and bioassays-guided approaches to aid in the preliminary screening, fractionation and purification of the targeted bioactive compounds. Eight pure fungal strains were successfully isolated from the fresh root and stem of the mangrove plant *A. lanata.* Rendering the bioactivities of the fungal extracts against *T.b. brucei*, two strains were further chosen for further isolation and chemical work. The objective of this study is to establish a metabolomics approach to target and pinpoint the bioactive secondary metabolites directly from the crude or initial chromatographic fractions, subsequently, averting the expensive and time-consuming bioassay work for every step of the isolation work.

2. MATERIALS AND METHODS

Fusarium sp. and *Lasiodiplodia theobromae* was isolated from the fresh root and stem (10 cm), respectively, of the mangrove plant *A. lanata* collected from Setiu Wetlands, Terengganu, Malaysia. The respective plant parts were packed and kept in a cold box and transported to the University of Strathclyde. Upon arrival, the material was washed under running tap water for a few minutes and cut into 2 cm x 2 cm segments. The plant tissue was immersed with 70% isopropanol in order to surface sterilize

the exposed external tissue and was rinsed with sterilized distilled water. The leaves were dissected to retrieve thin slices of the inner tissue parts, which were laid onto a malt nutrient agar (MA). Duplicate plates were prepared. Control malt nutrient agar plate was also prepared as a blank and left opened under microbiological safety cabinet BioMAT^2 (Medical Air Technology, UK) during the seeding process. The plates were incubated at 27 $\pm$ 2 °C (Vindon Scientific Ltd., UK) for 7-15 days. All morphologically different colonies were observed and isolated based on the colour of the colony, shape or texture of the mycelial pellicle. A 5 mm x 5 mm diameter plug was cut from the edge of the colony and placed in the middle of a new malt agar plate to establish a pure colony. The plates were incubated again for 7-15 days. The purity of the single strain was verified by visual examination. When colonies were not pure, the isolation step was repeated until a pure colony was achieved. Pure strains were re-inoculated and incubated for further taxonomical characterization by molecular biological methods.

3. EXPERIMENTAL

3.1 General Experimental Procedures

Structure determination of the isolated compounds was based on MS and NMR spectroscopy data. One dimensional NMR (1D NMR) data consisted of ^{1}H and ^{13}C NMR spectra captured using Jeol (^{1}H 400 MHz, ^{13}C 100.5 MHz, SIPBS, University of Strathclyde) and Bruker instruments (^{1}H 600 MHz, ^{13}C 150 MHz, Department of Pure and Applied Chemistry, University of Strathclyde) and was confirmed by two dimensional NMR (2D NMR) spectra such as HMQC or HSQC, HMBC, COSY and NOESY as well as comparisons with the literature. A pure sample was dissolved in 500 µL of a suitable deuterated solvent and transferred to 5 mm Norell NMR tube (Sigma-Aldrich, USA). Samples that were low in quantity were analysed in Shigemi tubes (Sigma-Aldrich, USA) with 180 µL of the appropriate deuterated solvent. Dimethyl sulfoxide-d_6, chloroform-d, acetone-d_6, and methanol-d3 bought from Sigma-Aldrich (USA) were the deuterated solvents used. The spectra were then processed with MestReNova-9.0 (MNova) 2.10 (Mestrelab Research, S.L, Santiago de Compostela, Spain). The optical rotation of optically-active compounds was measured with the digital polarimeter 341 (Perkin Elmer, USA) in which the pure compound was dissolved in in 2 mL of the suitable solvent (chloroform or acetone) to a concentration of 1 mg/mL.

3.2 DNA extraction, amplification, sequencing, and strain identification

The pure fungal strain was successfully isolated from the leaves of mangrove *A. lanata* and were identified by deoxyribonucleic acid (DNA) extraction, PCR amplification and sequencing by using polymerase chain reaction (PCR) with a universal ITS primers (Supporting Information; GenBank GQ856236 and GQ856237, respectively). The voucher specimens of all strains

were deposited at the Natural Product Metabolomics Laboratory (SIPBS, University of Strathclyde). The strain was chosen for further screening and optimized to produce bioactive metabolites using different media. The chemical profile at different growth phases was analyzed.

A small cube (1 cm x 1 cm) of active growing mycelium of the fungus was excised and transferred into a 2 mL of Eppendorf tube using a sterile scalpel. 100 µL of extraction solution (Sigma-Aldrich, UK) was subsequently added to the Eppendorf tube and briefly vortexed. The disk was thoroughly covered with the extraction solution. The sample was incubated at 95 °C for 10 mins. Then, 100 µL of dilution solution (Sigma-Aldrich, UK) was added to equal volumes of the extraction solution and vortexed to mix. The dissolved sample was stored at 2-8 °C prior to PCR.

The DNA extract was amplified by polymerase chain reaction (PCR) with a universal ITS primers. ITS1 was used as a forward primer and ITS4 as the reverse primer (Life Technologies, UK). PCR was carried out by using REDExtract-N-Amp PCR ReadyMix (Sigma-Aldrich, UK). Into a thin-walled PCR micro-centrifuge tube: 25 µL of REDExtract-N-Amp PCR ReadyMix, 18 µL of RNA-free water, 3 µL of ITS 1 and ITS 4 primers and 4 µL of fungal DNA were added to a volume of 53 µL. The components were mixed gently, centrifuged and the supernatant was collected then applied to the thermal cycler (Perkin Elmer, USA) using Genofun/Gfun TD1 PCR cycle. Initial denaturation was set at 95 °C, 15 mins for 1 cycle, followed by denaturation for 1 min (35 cycles). The temperature decreased at 56 °C for annealing, 0.5 min (35 cycles), later the temperature increased to 72 °C at 1 min (35 cycles) for extension. Final extension was continued for 10 mins (1 cycle) and hold at 4 °C prior to purification of the PCR products.

The PCR-amplified DNA was purified on 1% agarose gel using gel electrophoresis at 60 V for 45 minutes in Tris/Borate/EDTA (TBE) buffer. The mixture was heated in the microwave for 1 min 30 sec. Water was added until the reading was zero, 2 µL of 1% ethidium bromide solution was added as a staining agent. The solution was immediately poured into a gel electrophoresis plate and left for 15 min to solidify. The TBE buffer was then added and 15 µL of PCR-amplified DNA products were pipetted into the well. The 6 µL DNA ladder was pipetted into the other well as reference. At t=0, the voltage was turned down to 150 V and the voltage was increased to 60 V as the gel plate was allowed to run for 45 min. The stained DNA fragment was observed under UV camera then sliced from the agarose gel plate and transferred into an Eppendorf tube.

The PCR-amplified DNA was purified using GenElute Gel Extraction Kit (Sigma-Aldrich, UK). The sliced gel was mixed with the Gel Solubilisation solution, incubated at 50-60^{0}C for 10 min and vortexed for 2-3 min then mixed with isopropanol and centrifuged. The solubilized gel solution was loaded into the binding column and centrifuged for 1 min, discarding the flow-

through liquid and washed twice then incubated for 1 min at 37 °C followed by centrifugation to elute the product. The sequence analysis of the amplicons and the base sequence was performed through GenBank with the aid of the Basic Local Alignment Search Tool (BLAST) (http://blast.ncbi.nlm.nih.gov/Blast.cgi) using the 'BLASTN' option. Comparison of the base sequences with the National Centre for Biotechnology Information (NCBI) database, the best hit [24] confirmed the identities of the fungal strains. All fungal sequences were at least 98% identical to the best hit in the NCBI database [25]. The identified fungi were *Fusarium* sp. and *Lasiodiplodia theobromae* assigned with the accession numbers FJ487927 and KC960898, respectively.

3.4 Dereplication by using HRESI-LCMS

The dereplication study on the total crude extract and fractions of the samples were performed using HRESI-LCMS, and then processed with the MZmine software, an *in-house* macro coupled with the Dictionary of Natural Products (DNP) 2015 and AntiMarin 2012, a combination of Antibase and MarinLit, and SIMCA 14 (Umetrics AB, Umeå, Sweden). The procedure and program for HRESI-LCMS was set up as described below. The total crude extract of 1 mg/mL in methanol was analysed on an Accela HPLC (Thermo Scientific, UK) coupled with a UV detector at 280 and 360 nm and an Exactive-Orbitrap high-resolution mass spectrometer (Thermo Scientific, UK). A methanol blank was also analyzed. The column attached to the HPLC was a HiChrom, ACE (Berkshire, UK) C_{18}, 75 mm × 3.0 mm, 5 µm column. The mobile phase consisted of micropore water (A) and acetonitrile (B) with 0.1 % formic acid for each solvent. The gradient program started with 10 % B linearly increased to 100 % B within 30 mins at a flow rate of 300 µL/min and remained isocratic for 5 min before linearly decreasing back to 10 % B in 1 min. The column was then re-equilibrated with 10% B for 9 min before the next injection. The total analysis time for each sample was 45 mins. The injection volume was 10 µL and the tray temperature was maintained at 12 ˚C. High-resolution mass spectrometry was carried out in both positive and negative ESI ionization switch modes with a spray voltage of 4.5 kV and capillary temperature at 320 ºC. The mass range was set from *m/z* 150-1500 for ESI-MS range.

The mass spectral data was processed using the procedure by MacIntyre et al, which was established in the Natural Products Metabolomics Group Laboratory at SIPBS as described here [26, 27]. The LC-MS chromatograms and spectra were viewed using Thermo Xcalibur 2.1 or MZmine 2.10. Raw data were initially sliced into negative and positive data sets using the MassConvert software package from ProteoWizard (pwiz). The sliced data sets were subsequently exported into MZmine 2.10. The spectra were crop-filtered from 4 to 40 mins. The peaks in the samples and solvent and media blanks (where applicable) were detected using the chromatogram builder. Mass ion peaks were isolated using a centroid detector threshold that is greater

than the noise level set at 1.0E4 using an MS level of 1. The chromatogram builder was used with a minimum time span set at 0.2 min, and the minimum height and m/z tolerance at 1.0E4 and 0.001 *m/z* or 5.0 ppm, respectively. Chromatogram deconvolution was then performed to detect the individual peaks. The local minimum search algorithm (chromatographic threshold: 90 %, search minimum in RT range: 0.4 min, minimum relative height: 5 %, minimum absolute height: 3.0E4, minimum ratio of peak top/edge: 2, and peak duration range: 0.3-5 min) was applied. Isotopes were also identified using the isotopic peaks grouper (*m/z* tolerance: 0.001 m/z or 5.0 ppm, retention time tolerance: 0.2 absolute (min), maximum charge: 2, and representative isotope: most intense). The retention time normalizer (*m/z* tolerance: 0.001 *m/z* or 5.0 ppm, retention time tolerance: 5.0 absolute (min), and minimum standard intensity: 5.0E3) was used to reduce inter-batch variation. The peak lists were all aligned using the join aligner parameters set at *m/z* tolerance: 0.001 *m/z* or 5.0 ppm, weight for *m/z*: 20, retention time tolerance: 5.0 relative (%), weight for RT: 20. Missing peaks were detected using the gap-filling peak finder (intensity tolerance: 1.0 %, m/z tolerance: 0.001 m/z or 5.0 ppm, and retention time tolerance of 0.5 absolute (min). An adduct search was performed for both negative and positive mode. For ESI negative mode, formate adducts were searched for, (RT tolerance: 0.2 absolute (min), m/z tolerance: 0.001 m/z or 5.0 ppm, max relative adduct peak height: 30 %). A complex search was also performed with ionization method $[M-H]^-$. For ESI positive mode, adducts that were searched included Na+H, K+H, NH_4 and ACN+H. A complex search was performed with ionization method $[M+H]^+$, retention time tolerance: 0.2 absolute (min), *m/z* tolerance: 0.001 m/z or 5.0 ppm, and with maximum complex peak height of 50 %. The processed data set was then subjected to molecular formula prediction and peak identification. The data sets were exported to csv (comma delimited) to be imported to the *in-house* macro workstation. By using the macro, both the negative and positive data sets were imported for preparation followed by the removal of all media blanks and the samples. The macro combined all processed data from different media and samples and then prepared for the final data set to be imported to SIMCA 14 followed by the dereplication step using the Antimarin and DNP databases. The combined data set was imported into SIMCA 14 for multivariate analysis. Pareto scaling was applied. PCA and supervised OPLS-DA were used compare the metabolic profiles of different samples and to evaluate their unique secondary metabolites. The models were validated by a permutation test. The Y intercept (Q^2Y) on the permutation graph is a measure to check against overfitting. A clear indication that the model is valid and does not happen by coincidence is when the Q^2 values of the permuted Y models are less than zero on the permutation plot test. Moreover, the difference between Q^2 and R^2Y must be less than 0.3, indicating the absence of overfitting.

3.5 Isolation and purification on the bioactive metabolites

The pure fungal strains were inoculated onto a new agar plate and incubated for 8 days. The agar on which the fungi grew on was cut into small cubes and transferred into 40 x 1L containing rice media (100 g of rice: 100 mL of water) or 20 x 2 L of Erlenmeyer flasks (200 g of rice: 200 mL of water) which have been autoclaved before use and incubated at room temperature for 15 days. The metabolites were extracted twice with equal volumes of ethyl acetate to the aqueous phase, homogenized and filtered to give an organic phase which was then concentrated under vacuum rotary evaporator (Büchi, Switzerland) to afford the crude extract. The total crude extract was dissolved in any suitable solvent, mixed with Celite S (Sigma-Aldrich, Mexico) then fractionated by medium pressure liquid chromatography (Büchi, Switzerland) through gradient elution commencing with 100% hexane to 100% ethyl acetate for 20 mins, followed by 100% ethyl acetate to 30% ethyl acetate and 70% methanol for 30 mins at a flow rate of 50 mL/min. A silica column (VersaFlash/Supelco, UK) with dimensions of 4 x 150 mm and a particle size of 20-45 μm was used. The fraction collection volume was set at 100 mL/tube. TLC was carried out to monitor the separation profiles of the fractions and similar fractions were pooled together. The pooled fractions were concentrated under vacuum by a rotary evaporator to give 16 major fractions and were analyzed using HRESI-MS for dereplication study and tested for anti-trypanosomal activity. The active major fractions were subjected to further isolation and purification using conventional gravity column or by high-throughput flash chromatography (Grace Reveleris, USA and Biotage Isolera One, Sweden) which can be either normal or reverse phase fitted with the respective commercially available pre-packed column either from Reveleris USA or SNAP Sweden. The two flash chromatography instruments were used to isolate and purify the active fractions or small quantity of the crude extracts. The non-UV active metabolites were purified by using Grace, since dual detectors were coupled to the instrument. Whereas, the UV active metabolites were purified by using Biotage, since this machine able to detect the UV active compounds in the 200-400 nm range. Open column chromatography was used with various column sizes and silica gel 60 (Kieselgel 60), 0.035-0.070 mm (220-440 mesh ASTM) (Alfa Aesar, UK).

3.5.1 Isolation of secondary metabolites from Fusarium

Further isolation and purification on the active fractions was carried out, targeted and afforded compounds **1**, **2**, **3**, and **4** that contributed to the anti- trypanosomal activity. The active fractions were subjected to different chromatography techniques using by high-throughput flash chromatography as well as the conventional gravity column. Purification of fraction 4 yielded violet crystals of anhydrofusarubin (**1**, 7.3 mg). Further isolation on fraction 8 gave red crystals of javanicin (**2**, 5.7 mg) and fraction six gave dihydrojavanicin (**3**, 2.4 mg). Purification of fraction 11 gave red crystals of solaniol (**4**, 7.0 mg).

3.5.2. Isolation of secondary metabolites from L. theobromae

The active fractions were subjected to isolation and purification, yielding six pure compounds. Further purification of fraction LTRC15-6 and 8 gave (−)-*trans-axial*-4-hydroxymellein (**5**, 7.0 mg) and another congener of (−)-*cis-equatorial*-4-hydroxymellein (**6**, 8.7 mg), respectively. Meanwhile, several purifications of fraction LTRC15-8 gave (−)-5-hydroxymellein (**7**, 6.0 mg). Isolation work on fraction LTRC15-3 yielded the colourless crystals of (-)-mellein, (**8**, 11.0 mg).

3.6 Bioassays

MIC assays were performed for samples having greater than 90% inhibition at a concentration of 20 μM in the initial screening campaign. The MIC values of the isolated compounds against *T. b. brucei* were determined by averaging the results of two independent assays. The concentrations were averaged and converted to μM.

Meanwhile, the initial screening for cytotoxicity activity of the isolated compounds was performed on human normal prostatic epithelial cells (PNT2A) at 100 μg/mL. The % D of control was determined by averaging the results of three independent assays. In the initial screening, if the cell viability is less than 60%, a concentration response test at 0.3 to 300 μg/mL was carried on.

3.6.1 Anti-trypanosomal Assay:

The activity of the fungal extracts along with its pure compounds were tested *in vitro* against the blood stream form of *Trypanosomal brucei brucei* (*T. b. brucei*) S427. The activity of the samples was determined using the well-established Alamar blue™ 96-well microplate assay, in which the screening procedure was modified from the microplate Alamar blue assay [28], to determine drug sensitivity of African trypanosomes. The samples were initially screened at one concentration (20 μg/mL crude extracts or fractions, 20 μM for pure compounds) to determine their *in vitro* activity. Stock solutions of tested samples in DMSO (Fischer Scientific, UK) were prepared at concentrations of 10 mg/mL (extracts) or 10 mM for pure compounds. The concentration of DMSO should not exceed 0.5% of the final test solution. The 10 mg/mL stock solutions of the samples were diluted 1 in 10 with HMI-9 and 4 μL was pipetted into 96 μL HMI-9 in the 96-well plate. Sterility and DMSO control samples were placed in column 1 of the 96-well plates, test samples in columns 2 to 11 and a concentration range of suramin as a positive control in column 12. Trypanosomes were counted using a haemocytometer and diluted to a concentration of 3.0×10^4 trypanosomes per mL, and 100 μL of this suspension was added to each well of the assay plate with the exception of A1 well which contained the sterility control. The assay plate was incubated at 37 ºC, 5% CO_2 under humidified atmosphere for 48

hours. Later, 20 µL of Alamar blue was added and further incubated for 24 hours. Fluorescence was then determined using the Wallac Victor 2 microplate reader (Perkin Elmer, Cambridge, UK) (excitation: 530 nm, emission: 590 nm). The results were calculated as % of the DMSO control values.

Minimum inhibitory concentration values (MIC) were determined for pure compounds with less than 10% growth compared to the control values. MIC determinations were carried out in duplicate. Test solutions at 200 µg/mL were prepared in column 2 by pipetting 4 µL of 10 mg/mL test stock solution and 196 µL of HMI-9 medium into each well. 100 µL of HMI-9 medium was pipetted into columns 1 and 3 to 12, and serial 1:1 dilutions are carried out using a multi-channel pipette from columns 2 to 11. 20 µL of x 10 concentration of suramin was added to column 12 (different concentrations, ranging from 0.008 to 1.0 µM). An inoculum of 100 µL of trypanosomes at a concentration of 3.0 x 10^4 per mL was added to each well except A1, and the procedure continued as previously described [28] The MIC values were determined as the concentration calculated to have growth activity less than 5% of the control values.

3.6.2 Cytotoxicity Assay:

The pure compounds from endophytic fungi of mangrove plant *A. lanata* were tested for cytotoxicity *in vitro* against human normal prostatic epithelial cell line (PNT2A) derived from ECACC (Sigma-Aldrich, Dorset, UK).

The cytotoxicity activity of the pure compounds was determined using the well-established Alamar Blue™ redox-based 96-well microplate assay, in which the screening procedure was modified from [29]. PNT2A cells were seeded into 96-well microplate assay at density of 0.5 x 10^4 cells/well in 100 µL Dulbecco's modified Eagle's medium (DMEM; Invitrogen, Paisley, UK) and incubated at 37 ºC, 5% CO_2 with a humidified atmosphere for 24 hours. The tested compound was prepared at desired concentrations in DMEM solutions, while DMSO and Triton X as a negative and positive controls, respectively, were added into the microplate to give a total volume of 200 µL. The microplate plate was incubated at 37 ºC, 5% CO_2 with a humidified atmosphere for 24 hours, then 10 µL of Alamar blue was added. The microplate was further incubated for another 20 hours, then the fluorescence was measured using a Wallac Victor 2 microplate reader (Perkin Elmer, Cambridge, UK) (excitation: 530 nm, emission 590 nm). The results were calculated as % of the DMSO control values. IC_{50} values of the tested compounds were determined using Graph pad prism software.

4. RESULTS AND DISCUSSION

4.1 Dereplication of Small Scale Extracts of *Fusarium* sp. and *L. theobromae*

The OPLS-DA (Figure 2A) scores scatter plot showed the difference between small-scale active extracts (coloured blue) of *Fusarium* sp. (FRC15, FRC30, FLC7, FLC15, and FLC30) and *L. theobromae* (LTRC15). The inactive extracts (coloured green) are FRC7, LTRC7, LTRC30, LTLC7, LTLC15, and LTLC30. Meanwhile, from the S-loadings scatter plot (Figure 2B), metabolites can be predicted to be responsible for the anti-trypanosomal activity of the extract and be targeted for isolation work. From the *Fusarium* extracts, two discriminating metabolites found were at *m/z* 293.103 $[M–H]^-$ and 286.071 $[M+H]^+$, both of which gave a match from the database. The ion peak at *m/z* 286.071 $[M+H]^+$ was putatively identified as bostrycoidin previously isolated from *Fusarium solani, F oxysporum, F. decemcellulare, F. bostrycoides,* and *F. solani*. While the ion peak at *m/z* 293.103 $[M–H]^-$ matched with 7-O-demethylmonocerin earlier reported from *F. larvarum.* For *L. theobromae* bioactive extracts, the two discriminating metabolites were observed at *m/z* 337.258 $[M+H]^+$ and 552.392 $[M+H]^+$, which did not find any match from the database.

Table 1A. Yield and anti-trypanosomal activity of small-scale extracts and fractions (calculated as mean value of percentage viability) at concentrations of 20 µg/ mL. Highlighted extracts predict optimum fermentation conditions.

Fusarium sp.	Extract Yield (mg)	*T. b. brucei*, % D control
FRC7	63.8	94.0
FRC15	97.4	0.1
FRC30	103.2	-2.9
FLC7	24.2	-8.5
FLC15	72.6	-9.3
FLC30	84.3	-2.9
L. theobromae	Extract Yield (mg)	*T. b. brucei,* % D control
LTRC7	90.1	47.3
LTRC15	103.4	1.9
LTRC30	127.8	15.6
LTLC7	54.5	90.0
LTLC15	83.6	61.4
LTLC30	157.2	54.5

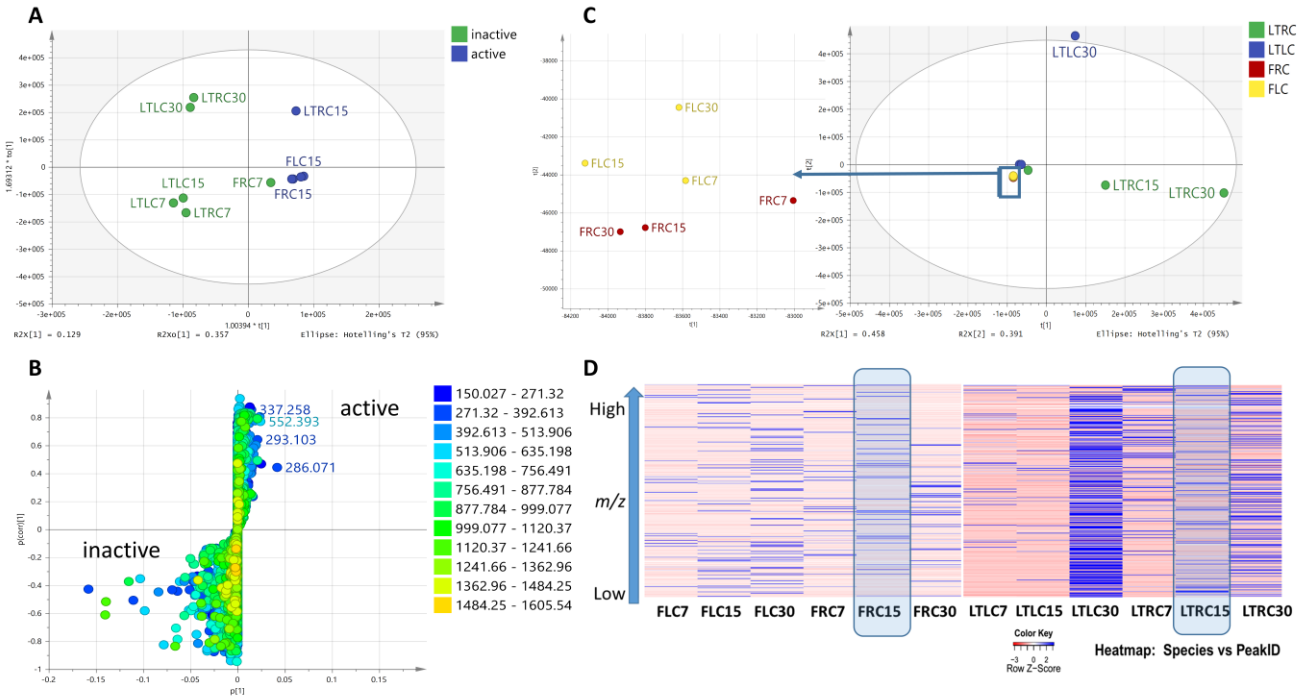

Figure 2. (**A**) OPLS-DA scores scatter and (**B**) S-loadings plot of small-scale extracts of *Fusarium* sp. and *L. theobromae* cultures ($R^2(Y) = 0.92$; $Q^2 = 0.576$; Q^2*(Y intercept)* from permutation test = −0.714). (**C**) PCA scores scatter plot ($R^2 = 0.849$; $Q^2 = 0.292$) and (D) heat map of HRMS data of small-scale extracts of *Fusarium* sp. and *L. theobromae* cultures. Highlighted column on heat map indicates best fermentation condition in terms of yield and bioactivity. Legend: FLC7 = *Fusarium* liquid culture-7 days; FLC15 = *Fusarium* liquid culture-15 days; FLC30 = *Fusarium* liquid culture-30 days; FRC7 = *Fusarium* rice culture-7 days; FRC15 = *Fusarium* rice culture-15 days; FRC30 = *Fusarium* rice culture-30 days; LTLC7 = *L. theobromae* liquid culture-7 days; LTLC15 = *L. theobromae* liquid culture-15 days; LTLC30 = *L. theobromae* liquid culture-30 days; LTRC7 = *L. theobromae* rice culture-7 days; LTRC15 = *L. theobromae* rice culture-15 days; LTRC30 = *L. theobromae* rice culture-30 days.

Amongst the small-scale extracts, cultures from days 15 and 30 for both media were considered for upscaling. The other parameters that needed to be considered were the shorter cultivation period and yield of the extract to have enough starting material for further isolation work (Table 1). A PCA model (Figure 2C) was also used to examine the variation and the diversity of the various extracts. However, the PCA model gave a low predictability score with $Q^2 = 0.292$. No significant variation can differentiate the *Fusarium* extracts. The differences between the extracts were visualized by using a heat map analysis of the HRMS datasets (Figure 2D). Amongst the *Fusarium* extracts, the fungus grown in 15 days rice cultures afforded more chemically diverse metabolites as represented by the blue bars between *m/z* 250 to 1000 Da, while it yielded less of the low molecular weight compounds at 150 to 250 Da. Interestingly, the 30 days rice culture of *L. theobromae,* despite of its increase in chemical diversity and extract yield, there was a significant loss of bioactivity. Based on the results of the heat map analysis of the mass spectral data (Figure 2D) and anti-trypanosomal activity, *Fusarium* sp. (FRC15) and *L. theobromae*

(LTRC15) grown in rice cultures incubated for 15 days were the optimum conditions for the production of the bioactive metabolites in these two fungi.

4.2 Dereplication, multivariate analysis, and isolation of bioactive metabolites of *Fusarium* sp. extracts and fractions

The dereplication study on the total crude extract of *Fusarium* sp. was performed by using the HRESI-LCMS data. The total ion chromatogram of the *Fusarium* sp. crude extract (Figure 3A) showed distribution of known and unknown compounds (Tables 2 and 3, respectively) present in FRC15 total extract. Most of the metabolites that gave a match from the database were produced from both marine and terrestrial fungi namely: *Sclerotinia libertiana, Gibberella fujikuroi, Epidermophyton floccosum, Fusarium* sp., *Aspergillus* sp., Basidiomycetes, *Pestalotiopsis* sp. and *Sphaeropsis sapinea* (Table 3). The *m/z* values and predicted formulas of unknown metabolites were also listed in Table 2.

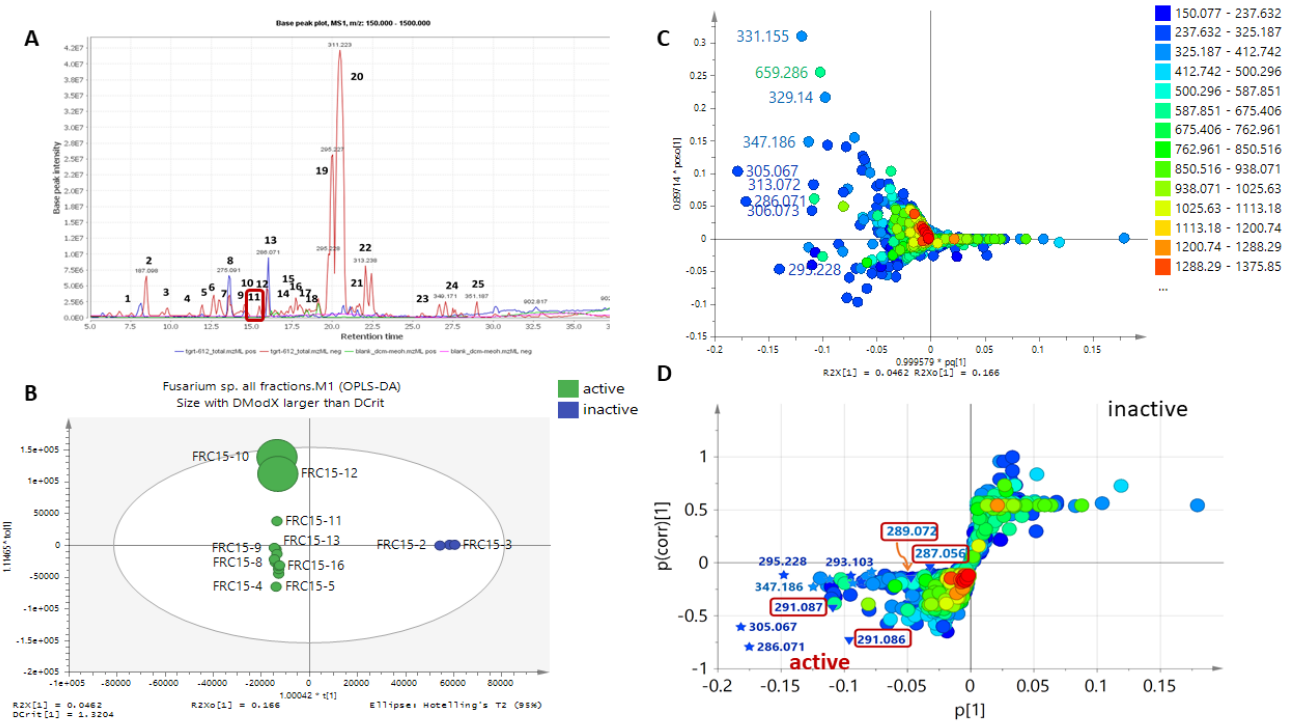

Figure 3. (**A**) Total ion chromatogram of the crude extract of *Fusarium* sp. grown in rice media for 15 days (FRC15) (blue and red represent positive and negative ionisation modes, respectively). Dereplication of numbered peaks is shown on Table 3. Boxed in red is the isolated compound javanicin. (**B**) OPLS-DA scores scatter plot of bioactive vs inactive *Fusarium* sp. fractions ($R^2(Y) = 0.998$; $Q^2 = 0.664$; Q^2(Y intercept) from permutation test = −0.15). (**C**) OPLS-DA loadings and (**D**) S-plot of bioactive vs inactive *Fusarium* metabolites. Metabolites designated with a star were those similarly observed on the TIC chromatogram as well as those discriminating metabolites during the initial fermentation procedure at *m/z* 293.103 $[M-H]^-$ and 286.071 $[M+H]^+$, while those in triangles and with boxed *m/z* represent the isolated compounds Their relative abundance in the active fractions are shown in Figure 4.

Table 3. List of compounds indicated on the total ion chromatogram for the crude extract of *Fusarium* sp. (FRC15) that were putatively identified using the Antimarin database. Highlighted rows represent compounds predicted to be anti-trypanosomally active by MVA as indicated with their MZmineIDs. Peak IDs used in this table correspond to those designated for the chromatogram shown on Figure 3A. *Isolated bioactive compound.

Peak ID	ESI modes /MZmineID	Rt (min)	MS (*m/z*)	Molecular weight	Chemical formula	Name	Tolerance (ppm)	Sources	Peak area
1	N	7.52	233.0819	234.0892	$C_{13}H_{14}O_4$	sclerin	-0.1035	*Sclerotinia libertiana*, *Aspergillus carneus*	1.04E+07
2	N	8.46	187.0976	188.1049	$C_9H_{16}O_4$	isoaspinonene	0.3467	*A. ochraceus*	8.81E+07
3	N	9.80	377.1607	378.1680	$C_{20}H_{26}O_7$	gibberellin A13	1.7686	*Gibberella fujikuroi*	2.14E+07
4	N	11.17	291.0511	292.0584	$C_{14}H_{12}O_7$	floccosic acid	2.0550	*Epidermophyton floccosum*	1.20E+07
5	N_5236	11.95	305.0667	306.2670	$C_{15}H_{14}O_7$	fusarubin	1.8790	*Fusarium solani*, *F. decemcellulare*, *F. marticipisi*, *F. javanicum*	2.21E+07
6	N_5758	12.59	329.1396	330.3750	$C_{19}H_{22}O_5$	gibberellin A11	1.9675	*Gibberella fujikuroi*	4.64E+07
7	N_3052	12.95	329.2334	330.2407	$C_{18}H_{34}O_5$	9,10,11-trihydroxy-(12*Z*)-12-octadecenoic acid	0.1969	Chinese truffle *Tuber indicum*	4.82E+07
8	P	13.57	275.0910	274.084	$C_{15}H_{14}O_5$	8-deoxyjavanicin	1.7348	*F. solani; "Munissi MUF2"*	8.60E+07
9	N_809	14.08	347.1864	348.1937	$C_{20}H_{28}O_5$	LL-S-491g; sphaeropsidin B	1.6057	*A. chevalierii* (Lederle S491), *Sphaeropsis sapinea*, *Diplodia mutila*,	2.49E+07
10	N_5770	14.31	329.0668	330.0741	$C_{17}H_{14}O_7$	bisdechlorogeodin	2.1585	*A. fumigatus*; (+): Penicillium *frequentans*; (-) *Oospora sulphurea.*	1.42E+07

XXX-XXX/14 $58.00+.00

11	P_2144	14.57	291.0862	290.0789	$C_{15}H_{14}O_6$	javanicin (**2**)*	1.5075	*F. solani*, *F. decemcellulare*	1.54E+07
12	N_2478	15.94	333.2073	334.2146	$C_{20}H_{30}O_4$	flexibilide	0.5461	Cnidaria; *Sinularia flexibilis*	5.09E+07
13	P_2560	16.02	286.0709	285.0637	$C_{15}H_{11}NO_5$	bostrycoidin	1.7338	*F. solani, F. oxysporum, F. decemcellulare*, *F. bostrycoides, F. solani*-purple	9.01E+07
14	N	16.44	327.2179	328.2251	$C_{18}H_{32}O_5$	SCH-725674	0.5532	*Aspergillus* sp.	2.46E+07
15	N	16.82	343.2127	344.2200	$C_{18}H_{32}O_6$	gallicynoic acid F	1.9340	Basidiomycete; *Coriolopsis gallica*	1.61E+07
16	N	17.20	325.2021	326.2094	$C_{18}H_{30}O_5$	pestalotiopsin B	0.3059	*Pestalotiopsis* sp. (endophytic fungus of *Taxus brevifolia*)	1.76E+07
17	N	18.01	347.1995	348.2068	$C_{18}H_{33}ClO_4$	plakortether C	0.0423	Porifera; *Plakortis simplex*	4.81E+07
18	N	18.39	307.1917	308.1989	$C_{18}H_{28}O_4$	sorokinianin	0.5743	*Bipolaris sorokiniana*	1.47E+07
19	N_499	19.96	295.2278	296.2350	$C_{18}H_{32}O_3$	(1*S*,2*R*)-3-oxo-2-(2*Z*-(1S,2R)-3-oxo-2-pentylcyclopentane-1-octanoic acid	0.3310	*F. oxysporum*	2.67E+07
20	N	20.49	311.2228	312.2301	$C_{18}H_{32}O_4$	filoboletic acid	1.7144	Fungus *Filoboletus* sp.	1.19E+09
21	N_2820	20.69	297.2435	298.2508	$C_{18}H_{34}O_3$	D-12-hydroxy-9-octadecenoid acid; ricinoleic acid	0.0901	Ascomycetes, Basidiomycetes	3.63E+07
22	N	22.07	313.2382	314.2458	$C_{18}H_{34}O_4$	6-hydroxy-4-oxo-octadecanoic acid	0.1789	*Hygrophorus discoxanthus*	1.87E+08
23	N	25.54	715.5327	716.5400	$C_{47}H_{72}O_5$	variabilin 5,9-tetracosadienoate	2.8351	Porifera *Ircinia felix*	6771285
24	P	27.50	395.2789	394.2724	$C_{23}H_{38}O_5$	15-acetoxyhexadecylcitraconic anhydride	0.7611	*A. wentii*	1.48E+07
25	N	28.97	351.1865	352.1937	$C_{18}H_{34}Cl_2O_2$	9,10-dichlorostearic acid	1.9680	*Verticillium dahliae*	2.96E+07

Table 2. Compounds present in the crude extract of *Fusarium* sp. (FRC15) that were unidentified using the Antimarin and DNP database.

ESI modes	Rt (min)	MS (*m/z*)	Molecular weight	Peak area
N	6.23	151.0400	152.0473	1.54E+07
P	8.12	164.1071	163.0998	3.85E+07
N	13.64	929.1953	930.2026	3.72E+07
N	14.60	923.1485	924.1558	2.60E+07
N	27.04	349.1709	350.1781	5.79E+07

The bioactivity test results on *Fusarium* sp. fractions showed that fractions 1 to 3 were inactive while fractions 4 to 12 exhibited strong anti-trypanosomal activity. Meanwhile, the OPLS-DA plot (Figure 3B) showed distinctive separation of fractions FRC15-10, 15-11 and 15-12 compared with the other bioactive fractions. Their dispersal from the other extracts reflected their unique chemical fingerprints. In Figure 3B, a larger sized symbol was used for observation points with DModX values twice as large as the DCrit values, as demonstrated by fractions FRC15-10 and 15-12. These extracts were then interpreted as moderate outliers. The DModX is the distance of the respective samples to the X plane of the model while DCrit is the critical distance to the model computed from the F-distribution to attain a 95% confidence interval limit. In simpler terms, at a significant level of 0.95, 95% of the observations should have DModX values less than the DCrit value at 1.302 in this model. Dcrit limit was set at 0.05. In this model, fractions FRC15-10 and 15-12 were shown to be different from the other extracts with respect to the correlation structure of its distinct chemical profile. The unique metabolites were indicated by $[M-H]^-$ ion peaks at *m/z* 331.155, 659.286, and 329.14, as shown on the OPLS-DA loadings scatter plot (Figure 3C). Dereplication results revealed that the ion peak at *m/z* 331.155 $[M-H]^-$ matched with the molecular formula $C_{19}H_{24}O_5$, putatively identified as pestalotiopsone A reported from *Pestalotiopsis* sp. The ion peak at *m/z* 329.140 $[M-H]^-$was dereplicated as a diterpene commonly found from *Sinularia* soft coral with a molecular formula of $C_{20}H_{24}O_5$. On the other hand, no hit was found for the ion peak at *m/z* 659.286 $[M-H]^-$.

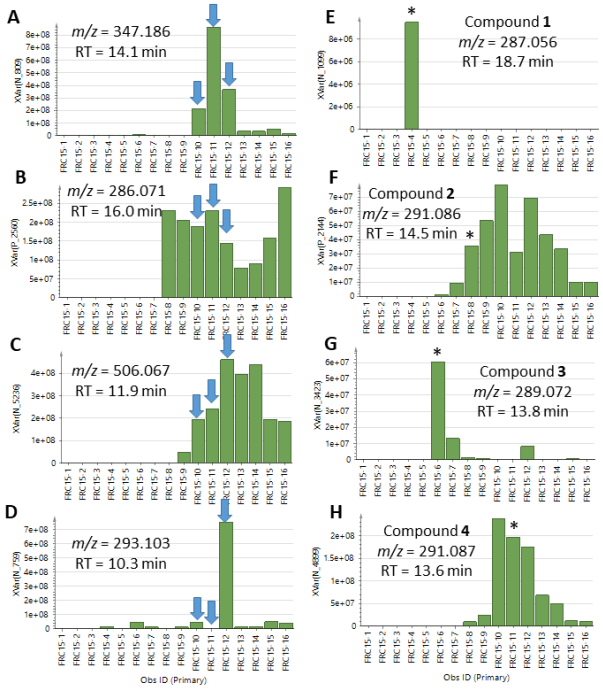

Figure 4. Relative abundance of target metabolites (A-D) and isolated naphthazarin derivatives in the bioactive fractions (E-H). Arrows indicate the occurrence of the target metabolites in the segregated fractions FRC15-10 to 12. Asterisk specifies the fraction from where the respective compounds were isolated. **A)** N_809: *m/z* = 347.186, RT = 14.1 min; **B)** P_2560: *m/z* = 286.071, RT = 16.0 min; **C)** N_5236: *m/z* = 506.067; RT = 11.9 min; **D)** N_759: *m/z* = 293.103, RT = 10.3 min; **E)** N_1099: anhydrofusarubin (**1**), *m/z* = 287.056, RT = 18.7 min; **F)** P_2144: javanicin (**2**), *m/z* = 291.086, RT = 14.5 min; **G)** N_3423: dihydrojavanicin (**3**), *m/z* = 289.072, RT = 13.8 min; **H)** N_4899: solaniol (**4**), *m/z* = 291.087, RT = 13.6 min.

Further investigation on *Fusarium* sp. extract FRC15 was carried out by evaluating the occurrence of the metabolites in the respective chromatographic fractions, which were correlated with their bioactivity against *T. b. brucei* (Figures 3C and 3D). It can be observed that not all peaks perceived on the TIC of the crude extracts listed on Table 3 were found on the active side of the S-plot. As shown on Figure 3D, metabolites designated with a star were those similarly observed on the TIC chromatogram as well as the discriminating metabolites found for the crude extracts at *m/z* 293.103 $[M-H]^-$ (7-O-demethylmonocerin) and 286.071 $[M+H]^+$ (bostrycoidin), while those in triangles and with boxed *m/z* values represent the isolated compounds. However, the peak signal for *m/z* 293.103 was not highlighted in the TIC (Figure 3A) due to the overlapping peaks in the crude extract of large scale batch. Further fractionation revealed the presence of this metabolite on the S-plot (Figure 3D). The discriminating metabolites targeted from the crude extract during the initial fermentation procedure were however not isolated due to their low yield in the active fractions. Although these two latter ion peaks were observed with good intensity, their detection was dependent on their capability to ionize and does not reflect their "true" concentration in the extract or the fraction. MVA is an unbiased approach in detecting the probable bioactive metabolites regardless of their concentrations in a fraction or crude

extract. The metabolomics approach has an advantage to the conventional way of phytochemical work done in the past where compounds were isolated according to their occurrence in a chromatogram. Albeit, very potent metabolites present at ng levels were detected, the limitation was the subsequent isolation work at which such low yielding compounds surpassed the limit of quantification. However, in this study, the MVA was able to guide the isolation work of the bioactive metabolites, which were not detected on the TIC. While mass spectrometry cannot be quantitative when the detection of respective compounds is dependent on their ionizing capability, NMR spectroscopy has the advantage of exhibiting the true ratios and a fingerprint of mixture metabolites in a crude extract or fraction. The NMR spectra of the active fractions of FRC15 were dominated by resonances typical for the naphthazarin derivatives as those of the exchangeable hydrogen bonded hydroxyl units at ca. 12 ppm rather than the 8 ppm resonance expected for a methine vicinal to a nitrogen unit in a pyridine system as in bostrycoidin. Instead, ion peaks at *m/z* 289.070 and 291.086 $[M+H]^+$ or 287.056 and 289.086 $[M–H]^–$ were isolated as well as elucidated as anhydrofusarubin (**1**) and javanicin (**2**), respectively, which have been previously described from *Fusarium* species, *F. decemcellulare* [30] and *F. solani* [31]. From the TIC peaks, only peak 11 could be isolated, which was later characterized as javanicin (**2**). Anhydrofusarubin was previously described from the fungus *F. solani* [32]. Javanicin (**2**) was earlier isolated from *F. javanicum* [33], another species of *Fusarium* sp. obtained as an aerial contaminant [34], and from *F. solani* isolated from pollen grain of *Pinus thumbergii* Parl [32], *Chloridium* sp.; an endophytic fungus from neem plant [35] and a sea fan-derived *Fusarium* [36]. However, in another report [37], the hydroxyl groups were attached at C-1 and C-4, respectively, which was proposed as dihydrojavanicin (**3**). Based on the spectral data and comparison with the literature, this compound was elucidated to be dihydrojavanicin (**3**) found at *m/z* 289.072 $[M–H]^–$, which had also been derived from the javanicin skeleton with a difference in positions of the carbonyl and hydroxyl substituents. However, this compound was also assigned the trivial name javanicin in the literature [37]. The metabolite with an ion peak at *m/z* 291.087 $[M–H]^–$ was recognized as solaniol (**4**), which was earlier isolated from *F. solani*; "munissi MUF2" [32, 36]. An ion peak at *m/z* 295.2280 $[M-H]^-$ was putatively identified as (1*S*,2*S*)-3-oxo-2(2*Z*-pentenyl)cyclopentane-1-octanoic acid which has been previously isolated from *F. oxysporum* [38]. The relative occurrence of the target metabolites and isolated compounds in the bioactive fractions and absence in the inactive fractions are shown on Figure 4.

4.3 Dereplication, multivariate analysis, and isolation of bioactive metabolites of *L. theobromae* extracts and fractions

The total ion chromatogram of the crude extract of *L. theobromae* LTRC15 (Figure 5A) presented the distribution of known and unknown compounds (Tables 4 and 5) present in LTRC15 total extract. These compounds were listed in Table 5 and were dereplicated using the AntiMarin and DNP database. Several of these identified metabolites were earlier isolated from other

endophytic fungi; these include asparvenone from *Aspergillus parvulus*, 1,3-dihydro-3,7-dihydroxy-5-methoxy-6-methyl-4-isobenzo-furancarboxylic acid from *Aspergillus duricaulis*, and viscumamide from *Paecilomyces* sp. isolated from mangroves. Some of the identified metabolites also have been isolated from marine endophytic fungi, bacteria, lichens, chordates, and sponges. Meanwhile, the *m/z* values and predicted formulas of unknown metabolites were listed in Table 4.

Table 4. Compounds present in the crude extract of *L. theobromae* (LTRC15) that were unidentified using the Antimarin and DNP database.

ESI modes	Rt (min)	MS (*m/z*)	Molecular weight	Peak Area
N	5.48	172.0971	173.1053	2.98E+08
N	5.97	151.0402	152.0475	4.39E+07
N	11.92	361.1870	362.1943	8.97E+08
N	15.57	519.2809	520.2882	1.51E+09
P	16.18	668.4230	667.4158	2.13E+08
N	18.54	835.4683	836.4756	3.59E+08
N	18.90	596.4028	597.4100	4.56E+07
N	19.84	610.4186	611.4259	5.31E+08
N	21.11	580.2950	581.3023	2.29E+08
P	27.90	535.3610	534.3537	1.45E+08

A dereplication study on the *L. theobromae* fractions was accomplished to investigate the metabolite profile of each fraction and its correlation with the bioactivity against *T. b. brucei* (Figure 5B). The loadings plot (Figure 5C) displayed the distribution of metabolites in the various fractions. The ion peaks at *m/z* 393.316 $[M+H]^+$, putatively identified as 24*R*-ergostatetraen-3-one was previously reported from *Dysidea herbacea* [39], 185.082 $[M-H]^-$ was identified as dihydroaspyrone from *Aspergillus ochraceus* [40], and 239.060 $[M-H]^-$ identified as coloratin B from *Xylaria intracolorata* [41]. Ion peaks at *m/z* 193.05 $[M-H]^-$ while overlapping on the loadings plots (Figures 5C and D) were identified and represents the isolated metabolites 4-hydroxymellein or also known as 4,8-dihydroxy-3-methylisochroman-1-one (**5** or **6**) and 5-hydroxymellein (**7**), respectively described from *Uvaria hamiltonii* [42] and *Penicillium* sp. [43]. Isolated compound **5** was designated as (−)-*trans-axial*-4-hydroxymellein. Compound **5** was earlier described by biotransformation of the marine bacterium *Stappia* sp. [44], as well as from the fungi *Aspergillus ochraceus, A. oniki, Seimatosporium* sp. and an endophytic fungus of the conifer tree *Canoplea elegantula* [45-48], *Uvaria hamiltonii* [42], *Apiospora camptospora* [49] and *Penicillium* sp. [43]. On the other hand, a (−)-*cis-equatorial*-4-hydroxymellein derivative (**6**) has been previously reported from the fungi *L. theobromae* [49], *A. ochraceus, Seimatosporium* sp. and the ascidian *Eudistoma vannamei* [45, 47, 50], *Uvaria hamiltonii* [42], *Cercospora taiwanensis* [51] and *Aspergillus melleus* [52, 53]. *Seimatosporium* sp. [47] was also conveyed to yield (−)-5-hydroxymellein

(**7**). It has also been described from the fungi *Septoria nodorum* [54] and *Botryosphaeria obtuse* [55, 56] and *Penicillium* sp. [43]. The identified ion peaks from the OPLS-DA loadings (Figure 5C) and S-plot (Figure 5D) representing the predicted bioactive metabolites were not perceivable from the TIC chromatogram shown in Figure 5A. For the similar reason, already mentioned above, MVA guided the isolation work of the bioactive metabolites, which were not detected on the TIC. The parent compound (−)-mellein (**8**) or 8-hydroxy-3-methylisochroman-1-one was also isolated. (−)-Mellein has been reported from an endophyte of the coniferous tree *Pezicula* sp. [57]. This compound was described for the first time from *Aspergillus melleus* [58], and previously reported from *Lasiodiplodia theobromae* [49], *Aspergillus ochraceus, Botryosphaeria obtusa* [45, 56], the mangrove ascomycete *Helicascus kanaloanus* [59], and a fungus causing the citrus disease, *Phoma tracheipilla* [60]. Mellein and its derivatives were isolated from fractions 3, 6, and 8 as indicated on the active side of the OPLS-DA scores plot (Figure 5B).

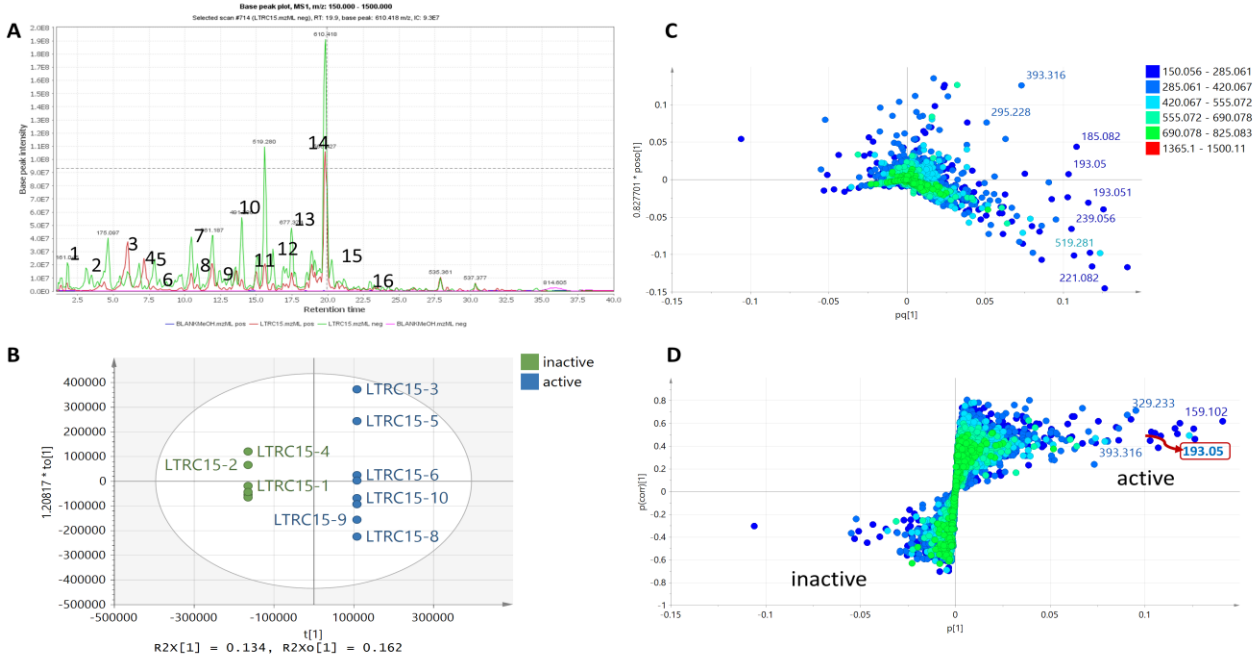

Figure 5. (**A**) Total ion chromatogram of the crude extract of *L. theobromae* grown in rice media for 15 days (FRC15) (green and red represent positive and negative ionisation modes, respectively). Dereplication of numbered peaks is shown on Table 5. (**B**) OPLS-DA scores scatter plot of bioactive vs inactive *L. theobromae* fractions ($R^2(Y)$ = 1.0; Q^2 = 0.743; Q^2(Y intercept) from permutation test = −0.0148). (**C**) OPLS-DA loadings and (**D**) S-plot of bioactive vs inactive metabolites. Boxed in red was the overlapping isolated isomers of hydroxymellein.

4.4 Bioactivity of isolated compounds

The isolated bioactive compounds were major metabolites present in the active fractions of *Fusarium* sp. and *Lasiodiplodia theobromae*. However, not all the predicted bioactive compounds were isolated. The isolated compounds represent 10-15% of total predicted active metabolites from both fungi. The isolated compounds **1**, **2**, **3**, and **4** exhibited significant activity against *T. b. brucei* and were comparable to suramin (Table 6).

Among the naphthazarin derivatives, solaniol (**4**) had the most potent activity against *T. b. brucei* with an MIC of 0.32 μM as also illustrated on the MVA S-plot (Figure 3D) when compared to the other isolated compounds. The next potent compound was javanicin (**2**) with an MIC of 0.60 μM, whereas dihydrojavanicin (**3**) exhibited less activity (MIC = 1.90 μM). Compounds **3** and **4** were the least toxic against PNT2A cells. Meanwhile, anhydrofusarubin (**1**), had an MIC of 1.20 μM. Notably, **1** and **2** showed similar moderate toxic effects against PNT2A cells. Mellein (**8**) and its derivatives **(5-7)** also showed activity against *T. b. brucei*, with (−)-5-hydroxymellein (**7**) possessing slightly higher potency (MIC of 2.40 μM) compared with **5**, **6** and **8.** The naphthazarin derivatives were relatively less toxic than the mellein congeners against PNT2A cells. The mellein congeners exhibited moderate toxicity.

5. CONCLUSION

The use of metabolomics tools assisted in the decision making which optimum fermentation conditions will be most appropriate for production of the bioactive metabolites and which fractions should be prioritized for further isolation work. Bioactive molecules were identified and targeted from the crude extracts. Dereplication study was used to screen the bioactive metabolites from the crude extracts prior to further scale up or purification work to avoid repetitive work of isolating known compounds with the same bioactivity already reported in the literature. The crude extracts obtained from the fungal mycelia were preliminarily screened by using HRESI-LCMS for bioactive molecules against *T. b. brucei* and were analysed by multivariate analysis such as PCA and OPLS-DA. Metabolomics and bioassay-guided isolation of potential anti-trypanosomal secondary metabolites were identified from the crude extracts of endophytic fungi isolated from the mangrove plant *A. lanata*, which included four naphthazarin-related naphthoquinones, and four dihydroisocoumarins (mellein and three derivatives), in which all compounds tested were active against the protozoa, *T. b. brucei*. The use of a metabolomics-guided approach has the great advantage to predict and target the bioactive metabolites regardless of their respective concentration in a fraction through multivariate analysis. In the conventional approach, isolation work will only be dependent on whatever was perceivable on a chromatogram with the risk of isolating the wrong compound that does not match the targeted bioactivity. The metabolomics approach can be a standalone method to target the bioactive compound during the several steps of chromatographic purification rather than re-submitting fractions for repetitive bioassay work resulting to loss of the compound. This study established the advantage of a metabolomics approach in natural products research for an efficient way to target the bioactive compound of interest in chromatographic isolation work.

Table 5. List of compounds indicated on the total ion chromatogram for the crude extract of L. *theobromae* (LTRC15) that were putatively identified using the Antimarin and DNP database. Highlighted rows represent compounds predicted to be anti-trypanosomally active by MVA. Peak IDs used in this table correspond to those designated for the chromatogram shown on Figure 5A. (Reported Sources; F-fungi, B-bacteria, M-mollusc, L-lichen, P-porifera)

	ESI modes	Rt (min)	MS (m/z)	Molecular weight	Chemical formula	Name	Tolerance (ppm)	Reported Sources	Peak Area
1	N	1.79	161.0454	162.1410	$C_6H_{10}O_5$	pentonic acid γ-lactone	2.2059	*Phycomyces blakesleeanus*	2.29E+08
2	N	3.50	181.0507	182.1730	$C_9H_{10}O_4$	6-ethyl-2,4-dihydroxybenzoic acid	0.1546	[F] *Penicillium baarnense*	3.12E+08
3	P	5.99	159.1018	158.1950	$C_8H_{14}O_3$	tetrahydro-4-hydroxy-6-propylpyran-2-one	1.2288	*Botryosphaeria rhodina* PSU-M35 and PSU-M114	1.01E+09
4	P	7.15	231.1592	230.3010	$C_{12}H_{22}O_4$	2,3-dihydroxydodecane-4,7-dione	0.3713	Basidiomycete; *Conocybe siliginea*	5.99E+08
5	N	7.89	221.0818	222.0891	$C_{12}H_{14}O_4$	asparvenone	1.8459	*Aspergillus parvulus*	5.02E+08
6	N	8.23	239.0560	240.0633	$C_{11}H_{12}O_6$	1,3-dihydro-3,7-dihydroxy-5-methoxy-6-methyl-4-isobenzofurancarboxylic acid	1.8471	*Aspergillus duricaulis*	2.14E+08
7	N	10.45	333.0770	334.1993	$C_{20}H_{14}O_5$	halenaquinol	1.9427	[P] *Xestospongia sapra*	7.42E+08
8	N	10.88	341.1606	342.1678	$C_{17}H_{26}O_7$	methyl 6-methoxydiperoxyhexadecaenoate	-0.0305	Porifera; *Plakortis* aff. *simplex*	3.57E+08
9	N	12.45	329.2334	330.4600	$C_{18}H_{34}O_5$	penicitide B	0.1045	*Penicillium chrysogenum*	3.05E+08

10	N	13.97	491.2860	492.2933	$C_{25}H_{40}N_4O_6$	glidobactin F; Bu-2867T-F	-1.9457	[M] *Polyangium brachysporum*	1.08E+09
11	P	14.97	281.1750	280.3590	$C_{16}H_{24}O_4$	tagetolone	2.9352	*Alternaria tagetica*	2.29E+08
12	N	16.16	649.3800	650.3873	$C_{32}H_{58}O_{13}$	glycolipid B; rhamnolipid B; R-1; acyl-dirhamnolipid-C10,C10	0.1219	[B] *Pseudomonas aeruginosa*; [B] rhizosphere bacterium*; Pseudomonas* sp. GRP3	8.56E+08
13	N	17.48	677.3750	678.3822	$C_{33}H_{58}O_{14}$	18-*O*-beta-D-glucopyranosyl-18*R*-hydroxydihydroalloprotolichesterinate-21-*O*-a-L-rhamnopyranoside	0.1905	[L] Lichens; *Acarospora gobiensis*, *Lecanora fructulosa*, *Peltigera canina*, *Rhizoplaca peltata*, *Xanthoparmelia camtschadalis*,	6.77E+08
14	P	19.82	566.4280	565.4208	$C_{31}H_{51}N_9O$	viscumamide	1.7923	endophytic *Paecilomyces* sp. from mangroves	1.98E+09
15	N	20.26	295.2278	296.2350	$C_{18}H_{32}O_3$	12-hydroxy-9*Z*,13*E*-octadecadienoic acid	1.4322	*Epichloe typhina*	4.75E+08
16	N	22.97	537.3282	538.3355	$C_{31}H_{46}N_4O_2S$	virenamide A	2.4383	Chordata; *Diplosoma virens*	1.14E+08

Table 6. Activities of the isolated compounds from *Fusarium* and *Lasiodiplodia* sp. against *T. b. brucei* and PNT2A cells.

		Cytotoxicity [b]	
Compound No.	**[a] MICs (µM)**	**% DMSO of control at 100 µg/mL**	**IC_{50} (µM)**
1	1.20	67.1	258.6
2	0.60	61.4	274.4
3	1.90	22.3	771.3
4	0.32	38.6	443.0
5	3.20	82.3	312.9
6	8.20	87.8	293.3
7	2.40	89.7	287.1
8	5.80	84.4	314.6
suramin	0.11	n.d	258.6
Triton X	n.d	0.082	

Compound No.	**IC_{50} (µg/mL) *T. b. brucei***	**IC_{50} (µg/mL) PNT2A cells**	**SI[c]**
1	0.173	74.48	431
2	0.089	81.22	915
3	0.276	223.68	812
4	0.047	129.36	2769
5	0.310	60.70	196
6	0.795	56.90	72
7	0.233	55.70	239
8	0.545	59.14	108
suramin	0.071	n.d	

[a] Each sample was tested in two independent assays against *T. b. brucei*, MIC values indicate the minimum inhibitory concentration of a compound/standard in µM necessary to achieve 90% growth inhibition. MICs (MIC < 10 µM - promising; 10 µM < MIC > 20 µM - moderate; 20 µM < MIC > 30 µM - marginal/weak; 30 µM < MIC > 40 µM - limited; MIC > 40 µM - no activity);

[b] Initial screening for cytotoxicity activity against human normal prostatic epithelial cells (PNT2A), % DMSO of control values (at 100 µg/mL) were determined by averaging of three independent assays results (n=3); [c, d] Positive controls; n.d.- not determined.

[c] Given the IC_{50} values for the PNT2A cells and for *T. b. brucei*, the selectivity index (SI) was calculated:

SI = (IC_{50} for mammalian cell line / IC_{50} for protozoan parasite)

If the IC_{50} for mammalian cell line PNT2A is > 90 µg/ml, the compound is classified as not cytotoxic. If the IC_{50} is between 2 and 89 µg/mL, the compound is classified as moderately cytotoxic. If the IC_{50} is < 2 µg/mL, the compound is classified as cytotoxic. This was based on the work plans of the Special Programme for Research and Training in Tropical Diseases (TDR), a global programme of scientific collaboration that helps facilitate, support and influence efforts to combat diseases of poverty. It is hosted at the World Health Organization (WHO), and is sponsored by the United Nations Children's Fund (UNICEF), the United Nations Development Programme (UNDP), the World Bank and WHO. https://www.who.int/tdr/grants/workplans/en/cytotoxicity_invitro.pdf. Accessed 21 May 2019.

CONFLICT OF INTEREST

The authors declare no conflict of interest.

FUNDING

We wish to thank the Ministry of Higher Education Malaysia for giving scholarship scheme to Noor Wini Mazlan.

ACKNOWLEDGEMENTS

The research described in this study have been done in SIPBS, University of Strathclyde. The authors would like to thank Dr. Tong Zhang for assisting in the mass spectrometry measurements and Mr. Craig Irving in the Department of Pure and Applied Chemistry for doing the NMR experiments, and Mr. Haji Muhamad Razali Salam for his help in collecting the plant samples.

REFERENCES

[1] Hyde, K.; Soytong, K., The fungal endophyte dilemma. *Fungal Diversity,* **2008**, *33*, 163-173.

[2] Nair, D.N.; Padmavathy, S., Impact of endophytic microorganisms on plants, environment and humans. *The Scientific World Journal,* **2014**, *2014*, 250693.

[3] Cribb, A.B.; Cribb, J.W., Marine fungi from Queensland. *Brisbane: University of Queensland Press,* **1955**.

[4] Kim, H.K.; Verpoorte, R., Sample preparation for plant metabolomics. *Phytochemical Analysis,* **2010**, *21*, (1), 4-13.

[5] Verpoorte, R.; Choi, Y.; Kim, H., NMR-based metabolomics at work in phytochemistry. *Phytochemistry reviews,* **2007**, *6*, (1), 3-14.

[6] Nielsen, J.; Oliver, S., The next wave in metabolome analysis. *Trends in Biotechnology,* **2005**, *23*, (11), 544-546.

[7] Wolfender, J.-L.; Marti, G.; Thomas, A.; Bertrand, S., Current approaches and challenges for the metabolite profiling of complex natural extracts. *Journal of Chromatography A,* **2015**, *1382*, 136-164.

[8] Horning, E.; Horning, M., Metabolic profiles: chromatographic methods for isolation and characterization of a variety of metabolites in man. *Methods in Medical Research,* **1970**, *12*, 369.

[9] Devaux, P.; Horning, M.; Horning, E., Benzyloxime derivatives of steroids. A new metabolic profile procedure for human urinary steroids human urinary steroids. *Analytical Letters,* **1971**, *4*, (3), 151-160.

[10] Grotewold, E., Plant metabolic diversity: a regulatory perspective. *Trends in Plant Science,* **2005**, *10*, (2), 57-62.

[11] Koehn, F.E.; Carter, G.T., The evolving role of natural products in drug discovery. *Nature Reviews Drug Discovery,* **2005**, *4*, (3), 206-220.

[12] Fiehn, O., Combining genomics, metabolome analysis, and biochemical modelling to understand metabolic networks. *Comparative and Functional Genomics,* **2001**, *2*, (3), 155-168.

[13] Berrueta, L.A.; Alonso-Salces, R.M.; Héberger, K., Supervised pattern recognition in food analysis. *Journal of Chromatography A,* **2007**, *1158*, (1), 196-214.

[14] Krug, D.; Zurek, G.; Revermann, O.; Vos, M.; Velicer, G.J.; Müller, R., Discovering the hidden secondary metabolome of *Myxococcus xanthus*: a study of intraspecific diversity. *Applied and Environmental Microbiology,* **2008**, *74*, (10), 3058-3068.

[15] Wold, H. In *Encyclopedia of Statistical Sciences*; John Wiley & Sons, Inc., **2004**.

[16] Hotez, P.J.; Molyneux, D.H.; Fenwick, A.; Kumaresan, J.; Sachs, S.E.; Sachs, J.D.; Savioli, L., Control of neglected tropical diseases. *New England Journal of Medicine,* **2007**, *357*, (10), 1018-1027.

[17] Brun, R.; Blum, J.; Chappuis, F.; Burri, C., Human african trypanosomiasis. *The Lancet,* **2010**, *375*, (9709), 148-159.

[18] Newman, D.J.; Cragg, G.M., Natural products as sources of new drugs over the 30 years from 1981 to 2010. *Journal of Natural Products,* **2012**, *75*, (3), 311-335.

[19] Gurnani, N.; Mehta, D.; Gupta, M.; Mehta, B., Natural Products: Source of Potential Drugs. *African Journal of Basic & Applied Sciences,* **2014**, *6*, (6), 171-186.

[20] Harvey, A.L.; Edrada-Ebel, R.; Quinn, R.J., The re-emergence of natural products for drug discovery in the genomics era. *Nature Reviews Drug Discovery,* **2015**, *14*, (2), 111-129.

[21] Ribeiro-Rodrigues, R.; dos Santos, W.G.; Zani, C.L.; Oliveira, A.B.; Snieckus, V.; Romanha, A.J., Growth inhibitory effect of naphthofuran and naphthofuranquinone derivatives on *Trypanosoma cruzi* epimastigotes. *Bioorganic and Medicinal Chemistry Letters,* **1995**, *5*, (14), 1509-1512.

[22] Morello, A.; Pavani, M.; Garbarino, J.A.; Chamy, M.C.; Frey, C.; Mancilla, J.; Guerrero, A.; Repetto, Y.; Ferreira, J., Effects and mode of action of 1,4-naphthoquinones isolated from *Calceolaria sessilis* on tumoral cells and *Trypanosoma* parasites. *Comparative Biochemistry and Physiology. Part C, Pharmacology, Toxicology & Endocrinology,* **1995**, *112*, (2), 119-128.

[23] Pérez-Castorena, A.L.; Arciniegas, A.; Villaseñor, J.L.; de Vivar, A.R., Furanoeremophilane derivatives from *Psacalium beamanii*. *Revista de la Sociedad Química de Mexico,* **2004**, *48*, 21-23.

[24] Sayers, E.W.; Barrett, T.; Benson, D.A.; Bolton, E.; Bryant, S.H.; Canese, K.; Chetvernin, V.; Church, D.M.; DiCuccio, M.; Federhen, S.; Feolo, M.; Geer, L.Y.; Helmberg, W.; Kapustin, Y.; Landsman, D.; Lipman, D.J.; Lu, Z.; Madden, T.L.; Madej, T.; Maglott, D.R.; Marchler-Bauer, A.; Miller, V.; Mizrachi, I.; Ostell, J.; Panchenko, A.; Pruitt, K.D.; Schuler, G.D.; Sequeira, E.; Sherry, S.T.; Shumway, M.; Sirotkin, K.; Slotta, D.; Souvorov, A.; Starchenko, G.; Tatusova, T.A.; Wagner, L.; Wang, Y.; John Wilbur, W.; Yaschenko, E.; Ye, J., Database resources of the National Center for Biotechnology Information. *Nucleic Acids Research,* **2010**, *38*, (Database issue), D5-D16.

[25] Taylor, D.L.; Houston, S. In *Fungal Genomics*; Springer, **2011**, pp 141-155.

[26] Macintyre, L.; Zhang, T.; Viegelmann, C.; Martinez, I.; Cheng, C.; Dowdells, C.; Abdelmohsen, U.; Gernert, C.; Hentschel, U.; Edrada-Ebel, R., Metabolomic tools for secondary metabolite discovery from marine microbial symbionts. *Marine Drugs,* **2014**, *12*, (6), 3416-3448.

[27] Abdelmohsen, U.R.; Cheng, C.; Viegelmann, C.; Zhang, T.; Grkovic, T.; Ahmed, S.; Quinn, R.J.; Hentschel, U.; Edrada-Ebel, R., Dereplication strategies for targeted isolation of new antitrypanosomal actinosporins A and B from a marine sponge associated-*Actinokineospora* sp. EG49. *Marine Drugs,* **2014**, *12*, (3), 1220-1244.

[28] Räz, B.; Iten, M.; Grether-Bühler, Y.; Kaminsky, R.; Brun, R., The Alamar Blue® assay to determine drug sensitivity of African trypanosomes (*Tb rhodesiense* and *Tb gambiense*) in vitro. *Acta Tropica,* **1997**, *68*, (2), 139-147.

[29] O'Brien, J.; Wilson, I.; Orton, T.; Pognan, F., Investigation of the Alamar Blue (resazurin) fluorescent dye for the assessment of mammalian cell cytotoxicity. *European Journal of Biochemistry,* **2000**, *267*, (17), 5421-5426.

[30] Medentsev, A.; Baskunov, B.; Akimenko, V., Formation of naphthoquinone pigments by the fungus *Fusarium decemcellulare* and their influence on the oxidative metabolism of the producer. *Biochemistry (USA),* **1988**.

[31] Tatum, J.H.; Baker, R.A., Naphthoquinones produced by Fusarium solani isolated from citrus. *Phytochemistry,* **1983**, *22*, (2), 543-547.

[32] Kimura, Y.; Shimada, A.; Nakajima, H.; Hamasaki, T., Structures of naphthoquinones produced by the fungus, *Fusarium* sp., and their biological activity toward pollen germination. *Agricultural and Biological Chemistry,* **1988**, *52*, (5), 1253-1259.

[33] Arnstein, H.R.V.; Cook, A.H., 189. Production of antibiotics by fungi. Part III. Javanicin. An antibacterial pigment from *Fusarium javanicum*. *Journal of the Chemical Society (Resumed),* **1947**, (0), 1021-1028.

[34] Chilton, W.S., Isolation and structure of norjavanicin. *The Journal of Organic Chemistry,* **1968**, *33*, (11), 4299-4300.

[35] Kharwar, R.; Verma, V.; Kumar, A.; Gond, S.; Harper, J.; Hess, W.; Lobkovosky, E.; Ma, C.; Ren, Y.; Strobel, G., Javanicin, an antibacterial naphthaquinone from an endophytic fungus of neem, *Chloridium* sp. *Current Microbiology,* **2009**, *58*, (3), 233-238.

[36] Trisuwan, K.; Khamthong, N.; Rukachaisirikul, V.; Phongpaichit, S.; Preedanon, S.; Sakayaroj, J., Anthraquinone, cyclopentanone, and naphthoquinone derivatives from the sea fan-derived fungi *Fusarium* spp. PSU-F14 and PSU-F135. *Journal of Natural Products,* **2010**, *73*, (9), 1507-1511.

[37] Bentley, R.; Gatenbeck, S., Naphthoquinone biosynthesis in molds. The mechanism for formation of mollisin. *Biochemistry,* **1965**, *4*, (6), 1150-1156.

[38] Miersch, O.; Bohlmann, H.; Wasternack, C., Jasmonates and related compounds from *Fusarium oxysporum*. *Phytochemistry,* **1999**, *50*, (4), 517-523.

[39] Kobayashi, M.; Krishna, M.M.; Ishida, K.; Anjaneyulu, V., Marine Sterols. XXII. Occurrence of 3-oxo-4, 6, 8(14)-triunsaturated steroids in the sponge *Dysidea herbacea*. *Chemical & Pharmaceutical Bulletin,* **1992**, *40*, (1), 72-74.

[40] Fuchser, J.; Zeeck, A., Secondary Metabolites by Chemical screening, 34.–aspinolides and aspinonene/aspyrone co-metabolites, new pentaketides produced by *Aspergillus ochraceus*. *Liebigs Annalen,* **1997**, *1997*, (1), 87-95.

[41] Quang, D.N.; Bach, D.D.; Hashimoto, T.; Asakawa, Y., Chemical constituents of the Vietnamese inedible mushroom *Xylaria intracolorata*. *Natural Product Research,* **2006**, *20*, (04), 317-321.

[42] Asha, K.N.; Chowdhry, R.; Hasan, C.M.; Rashid, M.A., Steroids and polyketides from *Uvaria hamiltonii* stem bark. *Acta Pharmaceutica-Zagreb-,* **2004**, *54*, (1), 57-64.

[43] Oliveira, C.M.; Silva, G.H.; Regasini, L.O.; Zanardi, L.M.; Evangelista, A.H.; Young, M.C.; Bolzani, V.S.; Araujo, A.R., Bioactive metabolites produced by *Penicillium* sp. 1 and sp. 2, two endophytes associated with *Alibertia macrophylla* (Rubiaceae). *Zeitschrift fur Naturforschung. C, Journal of biosciences,* **2009**, *64*, (11-12), 824-830.

[44] Feng, Z.; Nenkep, V.; Yun, K.; Zhang, D.; Choi, H.D.; Kang, J.S.; Son, B.W., Biotransformation of bioactive (-)-mellein by a marine isolate of bacterium *Stappia* sp. *Journal of Microbiology and Biotechnology,* **2010**, *20*, (6), 985-987.

[45] Cole, R.J.; Moore, J.H.; Davis, N.D.; Kirksey, J.W.; Diener, U.L., 4-Hydroxymellein. New metabolite of *Aspergillus ochraceus*. *Journal of Agricultural and Food Chemistry,* **1971**, *19*, (5), 909-911.

[46] Sasaki, M.; Kaneko, Y.; Oshita, K.; Takamatsu, H.; Asao, Y.; Yokotsuka, T., Studies on the compounds produced by molds: Part VII. Isolation of isocoumarin compounds. *Agricultural and Biological Chemistry,* **1970**, *34*, (9), 1296-1300.

[47] Hussain, H.; Krohn, K.; Schulz, B.; Draeger, S.; Nazir, M.; Saleem, M., Two new antimicrobial metabolites from the endophytic fungus, *Seimatosporium* sp. *Natural Product Communications,* **2012**, *7*, (3), 293-294.

[48] Findlay, J.A.; Buthelezi, S.; Lavoie, R.; Peña-Rodriguez, L.; Miller, J.D., Bioactive Isocoumarins and related metabolites from conifer endophytes. *Journal of Natural Products,* **1995**, *58*, (11), 1759-1766.

[49] Aldridge, D.; Galt, S.; Giles, D.; Turner, W., Metabolites of *Lasiodiplodia theobromae*. *Journal of the Chemical Society C: Organic,* **1971**, 1623-1627.

[50] Montenegro, T.G.C.; Rodrigues, F.A.R.; Jimenez, P.C.; Angelim, A.L.; Melo, V.M.M.; Rodrigues Filho, E.; de Oliveira, M.d.C.F.; Costa-Lotufo, L.V., Cytotoxic Activity of fungal strains isolated from the ascidian *Eudistoma vannamei. Chemistry & Biodiversity,* **2012**, *9*, (10), 2203-2209.

[51] Camarda, L.; Merlini, L.; Nasini, G., Metabolites of *Cercospora*. Taiwapyrone, an α-pyrone of unusual structure from *Cercospora taiwanensis*. *Phytochemistry,* **1976**, *15*, (4), 537-539.

[52] Garson, M.J.; Staunton, J.; Jones, P.G., New polyketide metabolites from *Aspergillus melleus*: structural and stereochemical studies. *Journal of the Chemical Society, Perkin Transactions 1,* **1984**, 1021-1026.

[53] Holker, J.S.; Simpson, T.J., Studies on fungal metabolites. Part 2. Carbon-13 nuclear magnetic resonance biosynthetic studies on pentaketide metabolites of *Aspergillus melleus*: 3-(1, 2-epoxypropyl)-5, 6-dihydro-5-hydroxy-6-methylpyran-2-one and mellein. *Journal of the Chemical Society, Perkin Transactions 1,* **1981**, 1397-1400.

[54] Devys, M.; Barbier, M.; Bousquet, J.-F.; Kollmann, A., Isolation of the (−)-(3R)-5-hydroxymellein from the fungus *Septoria nodorum*. *Phytochemistry,* **1994**, *35*, (3), 825-826.

[55] Venkatasubbaiah, P.; Chilton, W.S., Phytotoxins of *Botryosphaeria obtusa*. *Journal of Natural Products,* **1990**, *53*, (6), 1628-1630.

[56] Djoukeng, J.D.; Polli, S.; Larignon, P.; Abou-Mansour, E., Identification of phytotoxins from Botryosphaeria obtusa, a pathogen of black dead arm disease of grapevine. *European Journal of Plant Pathology,* **2009**, *124*, (2), 303-308.

[57] Schulz, B.; Sucker, J.; Aust, H.J.; Krohn, K.; Ludewig, K.; Jones, P.G.; Döring, D., Biologically active secondary metabolites of endophytic *Pezicula* species. *Mycological Research,* **1995**, *99*, (8), 1007-1015.

[58] Nishikawa, H., Biochemistry of Filamentous Fungi. II: A metabolic product of *Aspergillus melleus* Yukawa. Part I. *Journal of the Agricultural Chemical Society of Japan,* **1933**, *9*, (7-9), 107-109.

[59] Poch, G.K.; Gloer, J.B., Helicascolides A and B: new lactones from the marine fungus *Helicascus kanaloanus*. *Journal of Natural Products,* **1989**, *52*, (2), 257-260.

[60] Parisi, A.; Piattelli, M.; Tringali, C.; Di San Lio, G.M., Identification of the phytotoxin mellein in culture fluids of *Phoma tracheiphila*. *Phytochemistry,* **1993**, *32*, (4), 865-867.